doi:10.1016/j.jmb.2004.10.080 J. Mol. Biol. (2005) 345, 969–985

JMB

Available online at www.sciencedirect.com

SCIENCE DIRECT®

ELSEVIER

The Pre-tRNA Nucleotide Base and 2′-Hydroxyl at N(−1) Contribute to Fidelity in tRNA Processing by RNase P

Nathan H. Zahler, Lei Sun, Eric L. Christian and Michael E. Harris*

Department of Biochemistry Center for RNA Molecular Biology, Case Western Reserve University School of Medicine 10900 Euclid Avenue, Cleveland OH 44106-4973, USA

*Corresponding author

Fidelity in tRNA processing by the RNase P RNA from *Escherichia coli* depends, in part, on interactions with the nucleobase and 2′ hydroxyl group of N(−1), the nucleotide immediately upstream of the site of RNA strand cleavage. Here, we report a series of biochemical and structure–function studies designed to address how these interactions contribute to cleavage site selection. We find that simultaneous disruption of cleavage site nucleobase and 2′ hydroxyl interactions results in parallel reactions leading to correct cleavage and mis-cleavage one nucleotide upstream (5′) of the correct site. Changes in Mg^{2+} concentration and pH can influence the fraction of product that is incorrectly processed, with pH effects attributable to differences in the rate-limiting steps for the correct and mis-cleavage reaction pathways. Additionally, we provide evidence that interactions with the 2′ hydroxyl group adjacent to the reactive phosphate group also contribute to catalysis at the mis-cleavage site. Finally, disruption of the adjacent 2′-hydroxyl contact has a greater effect on catalysis when pairing between the ribozyme and N(−1) is also disrupted, and the effects of simultaneously disrupting these contacts on binding are also non-additive. One implication of these results is that mis-cleavage will result from any combination of active site modifications that decrease the rate of correct cleavage beyond a certain threshold. Indeed, we find that inhibition of correct cleavage and corresponding mis-cleavage also results from disruption of any combination of active site contacts including metal ion interactions and conserved pairing interactions with the 3′ RCCA sequence. Such redundancy in interactions needed for maintaining fidelity may reflect the necessity for multiple substrate recognition *in vivo*. These studies provide a framework for interpreting effects of substrate modifications on RNase P cleavage fidelity and provide evidence for interactions with the nucleobase and 2′ hydroxyl group adjacent to the reactive phosphate group in the transition state.

Keywords: ribonuclease P; ribozyme; pre-tRNA; tRNA processing

Introduction

The active sites of RNA enzymes, like their protein counterparts, involve networks of inter- and intramolecular interactions that are the basis for substrate recognition and catalysis.[1–3] The effects of disrupting these interactions by mutation or modification of enzyme and substrate residues can be complex due to the presence of conformational changes, or differences in the ground states or rate-limiting steps for different substrates.[4] Nonetheless, understanding such relationships among individual enzyme–substrate interactions is likely to be especially important for the molecular recognition by enzymes such as ribonuclease P (RNase P), ribonuclease MRP, the ribosome and the spliceosome, which bind multiple, structurally distinct RNA substrates.[5–7]

Bacterial RNase P is a ribonucleoprotein enzyme containing a single, highly conserved RNA, which

Present address: N. H. Zahler, Department of Chemistry, University of Michigan, Ann Arbor, MI 48109, USA.

Abbreviations used: RNase P, ribonuclease P; pre-tRNA, precursor tRNA; Mes, 2-morpholinoethanesulfonic acid; Pipes, piperazine-1,4-bis(2-ethanesulfonic acid).

E-mail address of the corresponding author: meh2@cwru.edu

is the catalytic subunit of the enzyme; and a small (ca 100 amino acid residues) protein that contributes to substrate binding by interacting directly with the pre-tRNA 5′ leader sequence.[8–11] The primary biological role of RNase P is removal of 5′ leader sequences from precursor tRNAs (pre-tRNAs), which requires that this single enzyme recognize all pre-tRNAs.[12–14] However, in bacterial species such as *Escherichia coli* and *Bacillus subtilis*, many pre-tRNA substrates do not possess the complete set of features known to be recognized by RNase P *in vitro*.[15–17] Therefore, a complete understanding of substrate recognition, cleavage site selection and catalysis by RNase P requires not only identification of individual enzyme–substrate interactions, but also an understanding of how these interactions may act together to ensure fidelity in tRNA processing.

Although a complete accounting of the interface between the RNase P RNA active site and the substrate cleavage site is not yet possible, cross-linking, chemical protection and structure–reactivity studies to date demonstrate interactions with the 3′RCCA sequence; the N(−1) nucleobase and 2′-hydroxyl group; and the N(+1)–N(+72) base-pair.[12,15,18] Additionally, phosphorothioate interference and metal switch experiments demonstrate that active site interactions also include metal ion coordination to the non-bridging oxygen atoms of the reactive phosphate group (Figure 1).[19–21] Importantly, modification of functional groups that are involved in these contacts weakens binding affinity, and in some cases significantly slows the rate of catalysis.

In addition to changes in affinity and catalytic rate, deletion or modification of functional groups important for RNase P substrate binding often results in mis-cleavage. Different pre-tRNAs are mis-cleaved at different sites, and loss of fidelity can result in processing within the acceptor stem, the 5′ leader sequence, or sometimes both. Although the factors that govern where mis-cleavage will occur are not entirely understood, structure–function studies using mis-cleavage as a readout provide important insights into P RNA–pre-tRNA interactions. In an important example, analysis of the

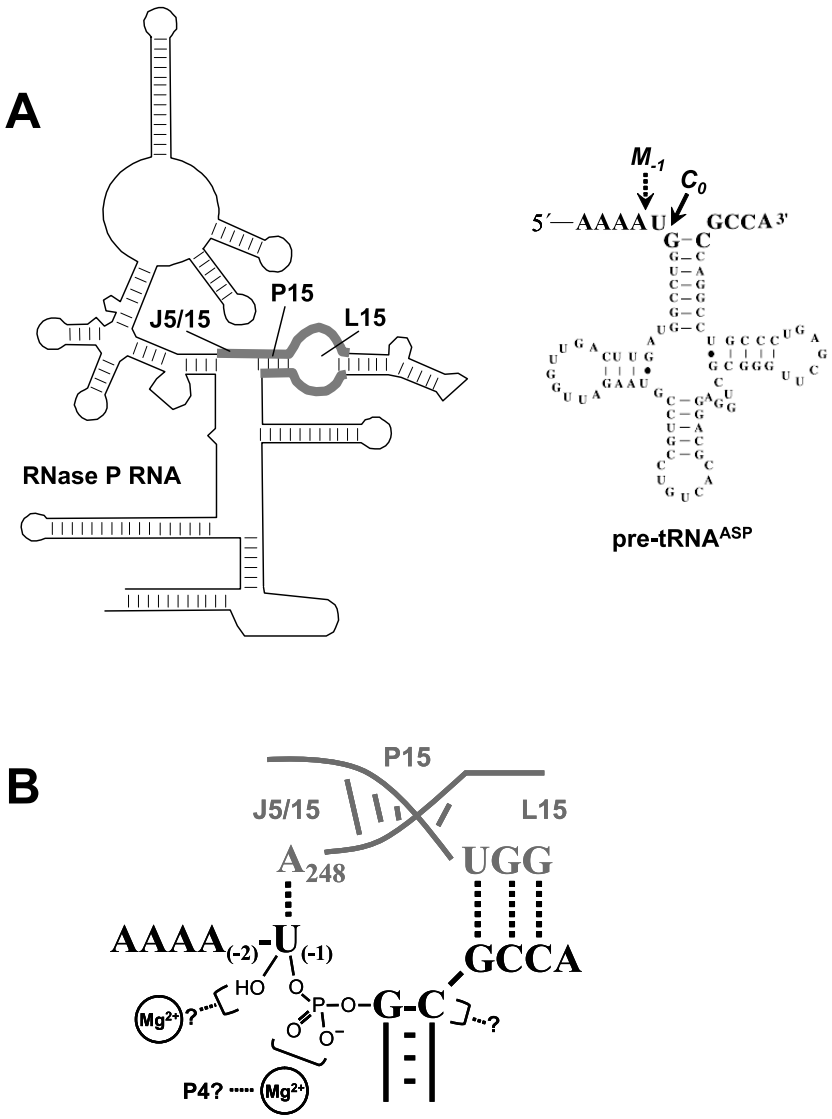

Figure 1. Interactions between P RNA and the pre-tRNA cleavage site. A, Secondary structure of *E. coli* P RNA (left) and a model pre-tRNA^{ASP} substrate from *B. subtilis* (right). Elements of P RNA structure highlighted in B, are shown by thick gray lines. The sites of correct cleavage, C_0, and the predominant site of mis-cleavage, M_{-1}, are indicated by arrows. Nucleotides that are recognition elements for P RNA are shown in bold. B, Illustration of interactions between P RNA and the pre-tRNA cleavage site. RNase P sequences are highlighted in gray and labeled according to A. Broken lines indicate individual pairing interactions, and brackets denote additional proposed interaction between the ribozyme and substrate.

effect on fidelity of compensatory mutations demonstrates an interaction between the substrate 3′RCCA sequence and the loop of helix P15 of P RNA (L15; Figure 1A).[22] Similar studies also provide evidence for a pairing interaction between the N(−1) nucleobase and J5/15.[15] Titration studies demonstrate that metal ion identity and concentration, as well as reaction pH can also influence cleavage site selection.[23–25] Moreover, changes in active site architecture due to changes in the nature of the 3′ RCCA and 5′ N(−1) interactions can affect the extent to which different combinations of metal ions lead to mis-cleavage. However, the relative importance of different active site contacts is only just coming into focus and the development of a general model to describe why and where mis-cleavage will occur has been difficult to achieve.

An additional challenge to understanding substrate recognition by P RNA is that the apparent effects of specific substrate modifications on reactivity and specificity can vary significantly for different substrates. For example, it is well established that the 2′-hydroxyl group adjacent to the site of substrate cleavage is an important recognition element for bacterial RNase P enzymes. However, reported binding defects for 2′-deoxy substitution at N(−1) range from non-existent to several hundred-fold.[25–27] Similarly, catalytic defects reported in the literature for removal of this functional group range from approximately 130-fold[25,28] to several thousand-fold.[26] In addition, 2′-deoxy modification at N(−1) alone does not generally result in loss of fidelity, yet, in combination with specific ribozyme mutations deletion of the 2′-hydroxyl group at N(−1) can lead to mis-cleavage.[15]

Some of the differential effects on cleavage fidelity and on the thermodynamic and kinetic contribution of individual residues are likely due to conformational changes during formation of the extensive interface between the ribozyme and the pre-tRNA cleavage site. Given the widespread observation and importance of conformational dynamics in other ribozymes,[29–32] it would be surprising if RNase P bound pre-tRNA in a simple lock and key type mechanism. Indeed, there is growing evidence that conformational changes contribute to a complex binding mechanism by RNase P RNA. Analyzing the inter-dependence of changes at N(−1) and N(+73) on multiple turnover reaction rate and specificity, Kirsebom and colleagues provide evidence that these nucleotides interact in the unbound substrate.[17] Additionally, they propose, based on the differential effects of mutations on k_{cat} and K_m values, that binding of a model hairpin substrate involves a pre-catalytic step in which this interaction is broken and new ribozyme–substrate interactions are formed. Conformational changes involving breaking base-pairs at the site of cleavage have also been proposed based on crosslinking and substrate-modification experiments.[33,34] Pan and colleagues showed that for the *B. subtilis* RNase P RNA, a 2′-deoxy modification at N(−1) slows the rate of catalysis at both the correct cleavage and mis-cleavage sites. This observation suggests that a contact to the 2′-hydroxyl group of N(−1) promotes a conformational change or docking step required for catalysis at both sites.[35,36] Thus, although significant progress has been made in defining RNase P–substrate interactions, a complete description of the active site environment, the mechanism of binding and the role of conformational changes have yet to be achieved.

To better understand substrate recognition by the RNase P ribozyme we analyzed the factors that influence fidelity in the processing of a model pre-tRNA^{Asp} substrate commonly used for kinetic and thermodynamic studies of bacterial RNase P. Previously, we found that disruption of the 248/N(−1) pairing interaction between the ribozyme and substrate together with a 2′-deoxy modification at N(−1) results in mis-cleavage one nucleotide 5′ of the correct site.[15] Here, we show that the single-turnover reaction kinetics of substrates engineered to disrupt N(−1) base and backbone interactions are consistent with parallel reactions leading to correct and mis-cleaved product. Titration studies reveal that changes in Mg^{2+} concentration and pH affect the extent of mis-cleavage, suggesting differences in the rate-limiting steps for the correct and mis-cleavage reaction pathways. Importantly, we also find that the apparent contributions of ribozyme interactions with the N(−1) nucleobase and 2′-hydroxyl to substrate binding affinity and catalytic rate are strongly coupled. Moreover, we find that individual substrate modifications that disrupt contacts to the N(−1) nucleobase, the N(−1) 2′-hydroxyl group, the reactive phosphate group, or the 3′-terminal RCCA motif do not by themselves result in a loss of fidelity. Rather, there is a threshold effect, whereby each of these modifications leads to an increased importance of remaining interactions for correct cleavage site selection, since any pair-wise combination consistently results in mis-cleavage. These results shed new light on the recognition of the pre-tRNA cleavage site by RNase P, and suggest that the redundant nature of interactions between the ribozyme and pre-tRNA cleavage site *in vitro* reflect the necessity for recognition of multiple substrates *in vivo*.

Results

Kinetics of mutant enzymes and substrates that disrupt N(−1) interactions reveal parallel pathways for formation of correct and mis-cleaved products

To examine the specificity of substrate binding by the *E. coli* RNase P ribozyme we used a model pre-tRNA^{ASP} substrate with a 5′ leader sequence 5′-AAAAU-3′. Derivatives of this substrate have been used for biochemical, thermodynamic and kinetic

studies of both *E. coli* and *B. subtilis* RNase P enzymes, providing a suitable backdrop for analysis of changes in enzyme fidelity.[9,11,15,37–44] Previous studies, as well as the current analysis (see below), show that pre-tRNA^{Asp} is cleaved exclusively at the correct site (C_0) by the native ribozyme, but that structure variants of the enzyme or substrate, in particular those that disrupt ribozyme interactions with N(−1), can lead to mis-cleavage one nucleotide 5′ to the correct site (M_{-1})[15] (Figure 1). An understanding of the mechanism by which RNase P discriminates between the C_0 and M_{-1} cleavage sites requires knowledge of the interactions and solution conditions that can influence cleavage site selection. Such studies require a general mechanistic framework within which to interpret the results of structure–function and titration studies. Previous studies of RNase P mis-cleavage show that cleavage at the C_0 and M_{-1} sites arise from structurally distinct enzyme–substrate complexes.[15,17] A simple model for formation of distinct ribozyme–substrate complexes under single-turnover conditions involves two parallel pseudo-first-order reactions as illustrated in Scheme 1:

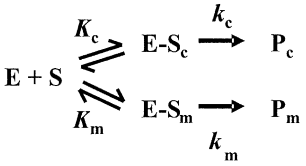

Scheme 1.

where E–S_c is the enzyme substrate complex that gives rise to cleavage at the correct site, generating product P_c; and E–S_m is the complex generating mis-cleaved product, P_m. A similar treatment was used by Pan and colleagues to describe mis-cleavage at three sites, including the C_0 and M_{-1} sites, of a pre-tRNA^{Phe} substrate by the *B. subtilis* P RNA ribozyme.[35,36] This mechanism predicts that in kinetic experiments the same apparent rate of cleavage, k_{obs}, will be observed for cleavage at both of the cleavage sites, and that the fraction of total cleavage which takes place at the correct site, F_c, will remain constant over time[35,45,46] (see Materials and Methods). However, more complex mechanisms are formally possible in which observed rates for the two sites differ, or there is a lag in the formation of one product.

Previously, we demonstrated that a substrate 2′-deoxy modification at N(−1) together with mutation of either N(−1) or position A248 in P RNA (the ribozyme residue with which N(−1) interacts) results in mis-cleavage at M_{-1}. To characterize the kinetics of correctly cleaved and mis-cleaved product formation, we examined reactions of native and A248U mutant ribozymes with substrates having either a 2′-deoxy uridine or 2′-deoxy adenosine at N(−1) (referred to as dU(-1) and dA(-1) pre-tRNA, respectively). The results of this analysis are shown in Figure 2. These combinations of ribozyme and substrate were chosen to give predominately correct cleavage (P RNA:dU[−1]) (Figure 2A), predominantly mis-cleavage (A248U:dU[−1]) (Figure 2B), or a mixture of products (P RNA:dA(-1) and A248U:dA(-1)) (Figure 2C and D). For all enzyme and substrate combinations examined, the fraction of total cleavage taking place at the correct site, F_c, remains constant over time. In addition, fitting the data for formation of the C_0 and M_{-1} products to a single-exponential function yields the same observed rate constant (Figure 2, and data not shown). This observation is consistent with the model shown in Scheme 1. Importantly, while Scheme 1 depicts the choice between correct cleavage and mis-cleavage taking place upon binding, this need not be the case. Cleavage site selection taking place through a conformational change subsequent to initial binding would also be consistent with these kinetic results. In either case, the simple model in Scheme 1 describing two parallel reactions provides a framework for interpreting experimental results, as well as assessing the limitations of quantitative analyses.

In Scheme 1, the fraction of substrate cleaved at the correct site is a function of the rates of chemical catalysis at both sites, as well as the equilibrium terms that describe the partitioning of the substrate into the E–S_c and E–S_m complexes (see also Materials and Methods). Thus, changes in F_c can arise from differences in the intrinsic rate of cleavage at either of the two sites, differences in binding affinity between the two complexes, or a combination of both. Given the observed rate constant and F_c it is possible to calculate the apparent rate of cleavage at a particular site (see Materials and Methods; equations (5) and (6)). However, as F_c is dependent on equilibrium binding terms, the magnitude of these rate constants will not be entirely determined by the cleavage step. Thus, quantitative analysis of F_c and apparent rates of cleavage and mis-cleavage must be undertaken with caution, since it is not possible to fully distinguish between effects on substrate binding and catalysis. Nonetheless, evaluation of these parameters provides an overall measure of the relative difference in the kinetics of the correct and mis-cleavage pathways. In addition, systematic analysis of the effects of substrate modifications on cleavage site selection provides a powerful way to survey for reaction conditions and ribozyme–substrate interactions that influence fidelity, which in turn provide insight into how the ribozyme insures fidelity.

Mg^{2+} and pH dependence of F_c suggest differences in the rate-limiting steps of the correct and mis-cleavage pathways

Given the model for parallel reactions in Scheme 1, it follows that the enzyme–substrate complexes E–S_c and E–S_m place different substrate

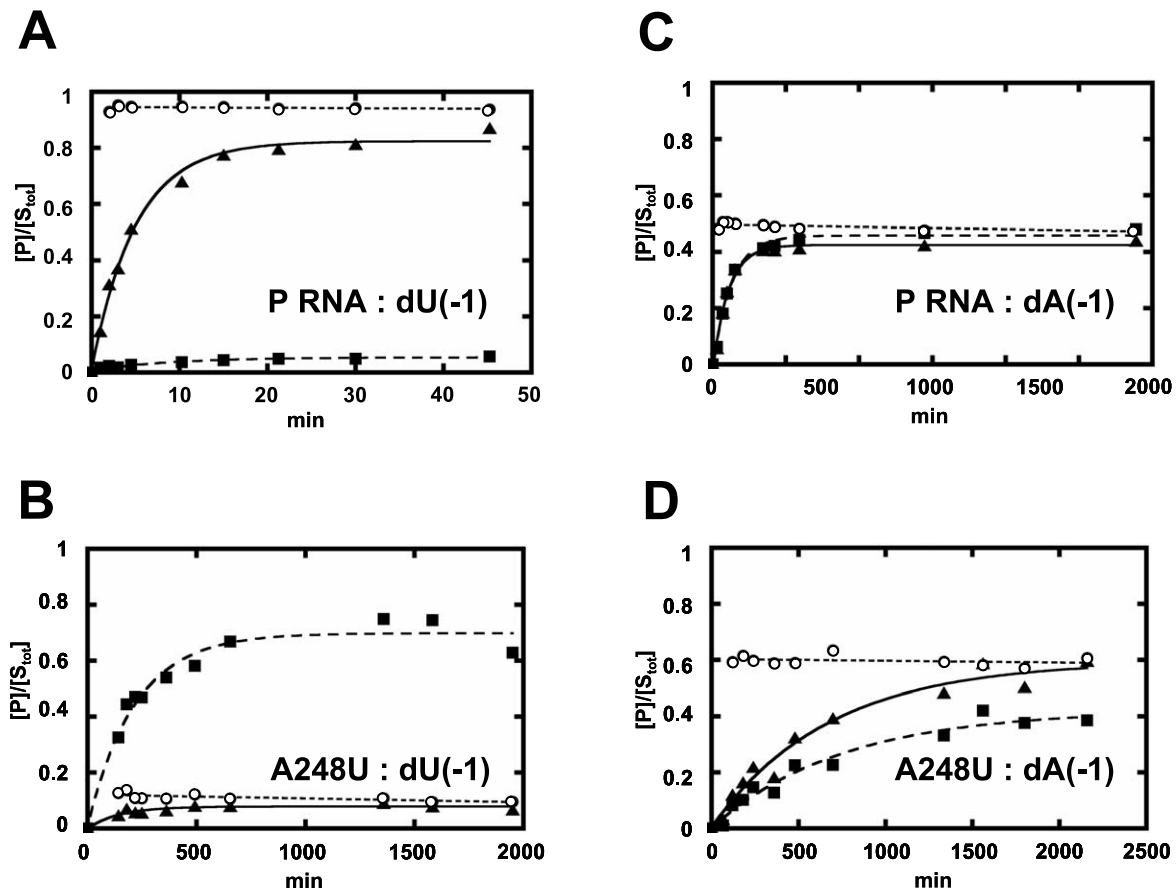

Figure 2. Kinetic analysis of cleavage at the C_0 and M_{-1} cleavage sites for pre-tRNA^{Asp}. A, Single turnover reactions for native RNase P RNA with the dU(-1) substrate. B, A248U mutant RNase P RNA with the dU(-1) substrate. C, Native RNase P RNA with the dA(-1) substrate. D, A248U RNase P RNA with the dA(-1) substrate. Plots show cleavage at the correct (C_0) site (triangles), the mis-cleavage site one nucleotide of the correct site (M_{-1}) site (squares), and the fraction of total cleavage taking place at the correct site (F_c; open circles). The fraction of substrate reacted is expressed as the ratio of product at a given time [P] to the total amount of substrate at the start of the reaction [S_{tot}].

phosphates in the RNase P active site. Additionally, previous mutational studies are consistent with a pairing interaction between N(−2), rather than N(−1), in the mis-cleavage complex.[15] These structural differences in the vicinity of the enzyme's active site have the potential to influence interactions between RNase P and essential magnesium (Mg^{2+}) ion and hydroxide cofactors, and to alter the rate-limiting step for catalysis. Therefore, changes in solution conditions could differentially affect the observed second-order rates ($k_{1,app}$; see Materials and Methods) for cleavage at the C_0 and M_{-1} sites. This, in turn, would cause a change in the fraction of substrate that is correctly cleaved, F_c.

RNase P RNA requires divalent metal ions to facilitate both substrate binding and catalysis.[39,47–50] Phosphorothioate interference rescue experiments indicate that metal ion interactions with the *pro*-R_P non-bridging oxygen atom of the reactive phosphate group contribute to catalysis.[19,21] Given the potential for structural differences between E–S_c and E–S_m, it seemed likely that they might differ with respect to Mg^{2+} binding. In addition, given its proximity to the cleavage site, disruption or alteration of the A248/N(−1) interaction could also weaken the binding of one or more functionally important magnesium ions. In such a case, it might be possible to influence cleavage site selection by changing the Mg^{2+} concentration.

Figure 3 shows a plot of F_c as a function of Mg^{2+} concentration for the P RNA:dU(-1), P A248U:dA(-1) and P RNA:dA(-1) enzyme/substrate combinations. At relatively low Mg^{2+} concentration, additional metal ion results in greater correct cleavage of all enzyme and substrate combinations with maximum values of F_c occurring at ca 10 mM for P RNA:dU(-1) and ca 25 mM for P RNA:dA(-1). At higher concentrations, however, increasing Mg^{2+} concentration causes an increase in the relative level of mis-cleavage. This pattern of cleavage site selection suggests that the pathway leading to cleavage at the C_0 site exhibits a greater apparent affinity for Mg^{2+} than the pathway leading to cleavage at the M_{-1} site. In this model, the cleavage at the C_0 site would be favored at low Mg^{2+} concentrations due to tighter binding. However, increasing Mg^{2+} concentrations increase the apparent rate of cleavage at the M_{-1} site due to a

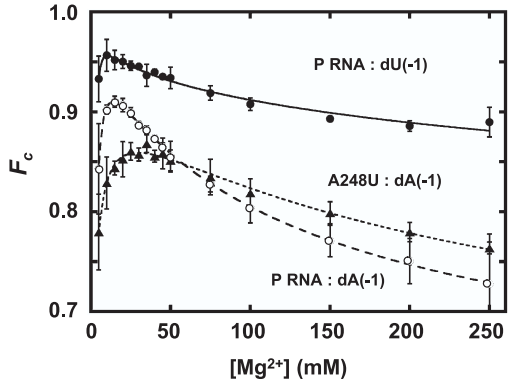

Figure 3. Mg^{2+} dependence of cleavage site selection. F_c is plotted as a function of Mg^{2+} concentration for native RNase P RNA and dU(-1) substrate (filled circles); native RNase P RNA and dA(-1) substrate (open circles); and the A248U mutant RNase P RNA with dA(-1) substrate (triangles). Curves are fit to equation (7) (see Materials and Methods). Reactions were carried out under standard reaction conditions at pH 7.8, using annealed substrates and with the given concentrations of Mg^{2+}. Error bars represent the standard deviation of a minimum of three independent trials. For points where no error bars are visible, standard deviations are less than ± 0.003.

weaker affinity of the E–S_m complex for metal ions, leading to the observed decrease in F_c.

To further explore this hypothesis, we fit the data in Figure 3 to a model describing the influence of Mg^{2+} on F_c, given the general mechanism in Scheme 1 and allowing for a cooperative dependence of cleavage at both the C_0 and M_{-1} sites on Mg^{2+} concentration (see Materials and Methods; equation (7)). Fitting the data to this model allows estimation of the apparent affinity and cooperativity of binding of Mg ions for the correct and mis-cleavage pathways that could shed light on structural or kinetic differences between them. Table 1 lists apparent values for $K_{1/2}^{Mg}$ and Hill coefficient (n_c and n_m) from reactions of the native ribozyme with the dU(-1) and dA(-1) substrates, and the A248U mutant with the dA(-1) substrate. Importantly, values of $K_{1/2}^{Mg}$, n_m and n_c determined from F_c are derived from the Mg^{2+} dependence of the apparent second-order rate constants for cleavage at the C_0 and M_{-1} sites (see Materials and Methods).

The data shown in Table 1 display two important differences between the correct and mis-cleavage pathways. First, the mis-cleavage pathway exhibits a significantly lower apparent affinity and decreased cooperativity for Mg^{2+} binding than the correct pathway. If the two pathways share the same rate-limiting step, then it is likely that structural differences between the E–S_m and E–S_c complexes are the basis for the weaker concentration dependence on metal ions. Alternatively, it is possible that the rate of mis-cleavage reflects, or is influenced by, a different rate-limiting step that displays different metal ion concentration dependence. A second important aspect of the data is the similarity in the parameters for Mg^{2+} dependence of the correct cleavage pathway for the ribozyme–substrate combinations tested. This result suggests that changes in the geometry of the A248/N(−1) interactions do not engender large changes in Mg^{2+} binding affinity.

It is well established that the rate of cleavage by the RNase P ribozyme increases with increasing pH and displays log–linear dependence with a slope of 1.[26] The pH dependence of P RNA is believed to arise from the dependence of phosphodiester hydrolysis on hydroxide concentration,[51,52] and is therefore taken to indicate that chemistry is rate limiting.[6,50] However, the correct cleavage and mis-cleavage pathways observed with A248 mutants and N(−1)-deoxy substrates may involve rate-limiting steps upstream of chemistry, which would alter the observed pH dependence. If so, then changes in pH will differentially affect the rates of the correct cleavage and mis-cleavage pathways, altering the observed level of mis-cleavage.

Figure 4 shows a plot of F_c between pH 5.5 and pH 7.8 for native P RNA and the A248U mutant ribozyme in combination with dU(-1) and dA(-1) substrates. For native P RNA and the A248U mutant ribozymes combined with the dU(-1) substrate, we observed no influence of pH on cleavage site selection. Notably, these combinations show strong preferences for correct cleavage, for the native enzyme, or for mis-cleavage at the M_{-1} position, with the A248U mutant. In contrast, combinations of the native and A248U mutant ribozymes with the dA(-1) substrate lead to moderate levels of mis-cleavage at low pH, yet increasing the pH from pH 5.5 to pH 7.8 results in a significant increase in the F_c value. A simple explanation for this result is that for these combinations of enzyme and substrate, the correct cleavage pathway has a greater pH dependency than the mis-cleavage pathway. Such differences in the pH dependency could arise from different rate-limiting steps for the two pathways, or differences

Table 1. Apparent affinity and cooperativity for the Mg^{2+} dependence of cleavage at the C_0 and M_{-1} sites

Enzyme	Substrate	$K_{1/2\,c}^{Mg}$ (mM)	n_c	$K_{1/2\,m}^{Mg}$ (mM)	n_m
Native	dU(-1)	9±2	2.0±0.3	120±60	0.8±0.2
Native	dA(-1)	10±2	2.3±0.3	280±20	0.8±0.04
A248U	dA(-1)	33±7	1.6±0.2	120±40	1.1±0.3

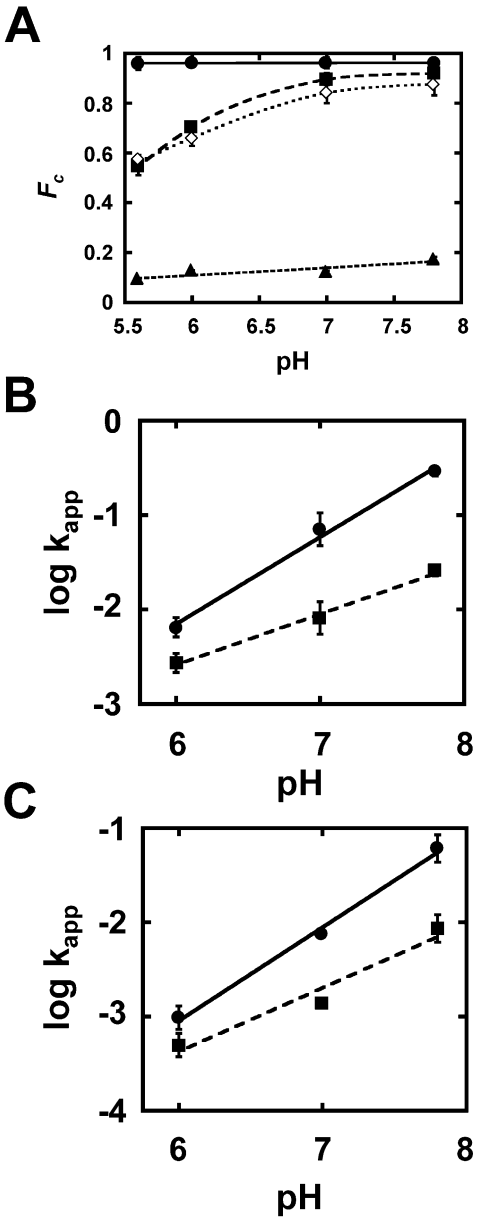

Figure 4. pH dependence of F_c. A, Effect of pH on F_c for the native ribozyme and dU(-1) substrate (circles), the native ribozyme and dA(-1) substrate (squares), the A248U mutant ribozyme and dU(-1) substrate (triangles) and the A248U ribozyme with the dA(-1) substrate (diamonds). Reactions were carried out under standard reaction conditions at the indicated pH. Lines connecting points are included only for convenience and are not meant to indicate a curve fit to a model. Error bars indicate the standard deviation of at least three independent trials. Points where no error bars are visible have a standard deviation of less than ± 0.01. B, Plot of log $k_{app,c}$ (circles) and $k_{app,m}$ (squares) *versus* pH for the native ribozyme/dA(-1) combination. Curve fits indicate slopes of 0.92 ± 0.08 for cleavage at the C_0 site and 0.54 ± 0.04 for cleavage at the M_{-1} site. C, Plot of log $k_{app,c}$ (circles) and $k_{app,m}$ (squares) *versus* pH for the A248U mutant ribozyme combined with the dA(-1) substrate. Slopes are 0.99 ± 0.07 for cleavage at the C_0 site and 0.67 ± 0.15 for cleavage at the M_{-1} site. In both B and C, error bars represent the standard deviation of three independent trials. For points where no error bar is visible, the standard deviation is less than ± 0.03 log unit.

in the structure or metal ion requirements for formation of the two enzyme–substrate complexes.

To evaluate this interpretation, we examined the pH dependence of the apparent rate of cleavage at the two cleavage sites. Given the model for cleavage site selection in Scheme 1, it is possible to calculate apparent first-order rates for correct cleavage ($k_{app,c}$) and mis-cleavage ($k_{app,m}$; see Materials and Methods).[35,36] The dependence of $k_{app,c}$ and $k_{app,m}$ on pH are shown in Figure 4B and C. For both enzyme–substrate combinations, we observe that the pH dependencies of $k_{app,c}$ and $k_{app,m}$ are log–linear, consistent with phosphodiester hydrolysis being either partially or completely rate limiting for both pathways. However, for both enzyme–substrate combinations, the apparent rate of reaction at the correct site, $k_{app,c}$ shows a slope of ca 1 while $k_{app,m}$ shows a slope of ca 0.5–0.6. The reduced pH dependence of $k_{app,m}$ is consistent with additional slow steps upstream of the hydrolysis step in the mis-cleavage pathway.

Recognition of the 2′-hydroxyl group adjacent to the reactive phosphate in both the correct (E–S_c) and mis-cleavage (E–S_m) complexes

Previous analyses by Pan and colleagues demonstrated that deletion of the 2′-hydroxyl group at N(−1) decreased the rate of cleavage at both the C_0 and M_{-1} sites in a pre-tRNA^{Phe} substrate. However, deletion of the 2′-hydroxyl group at N(−2) had no effect on rates of correct or incorrect processing, suggesting that the 2′-hydroxyl group of N(−1) was contacted in both the E–S_c and E–S_m complexes. To determine if the 2′-hydroxyl group adjacent to the dominant M_{-1} mis-cleavage site of the pre-tRNA^{Asp} substrate used here is contacted in the E–S_m complex, we analyzed the cleavage pattern of a substrate bearing 2′-deoxy modifications at both N(−1) and N(−2). If the 2′-hydroxyl group of N(−2) is indeed contacted in the mis-cleavage complex, its removal is expected to specifically slow the rate of cleavage at the M_{-1} site relative to the C_0 site. This would, in turn, increase F_c, resulting in an apparent rescue of cleavage at the correct position for the N(−1), N(−2)-dideoxy substrate compared to an N(−1)-deoxy substrate.

The results of 2′-deoxy modification at N(−2) are shown in Figure 5. Cleavage of all ribo, dU(-1) and dU(-1),dA(-2)-dideoxy substrates by the native ribozyme results in predominantly correct cleavage. Apparent changes in the mobility of these products result from the ability of high-percentage gels to resolve oligonucleotides that differ in base and backbone composition. Unlike the native ribozyme, however, the pattern of cleavage of these substrates by the A248U mutant is clearly altered by the introduction of the 2′-deoxy modification at N(−2). A248U cleavage of an all-ribo substrate results in only correct cleavage, while the N(−1)-deoxy substrate shows 87% mis-cleavage at pH 7.8 as observed previously. However, the 2′-deoxy

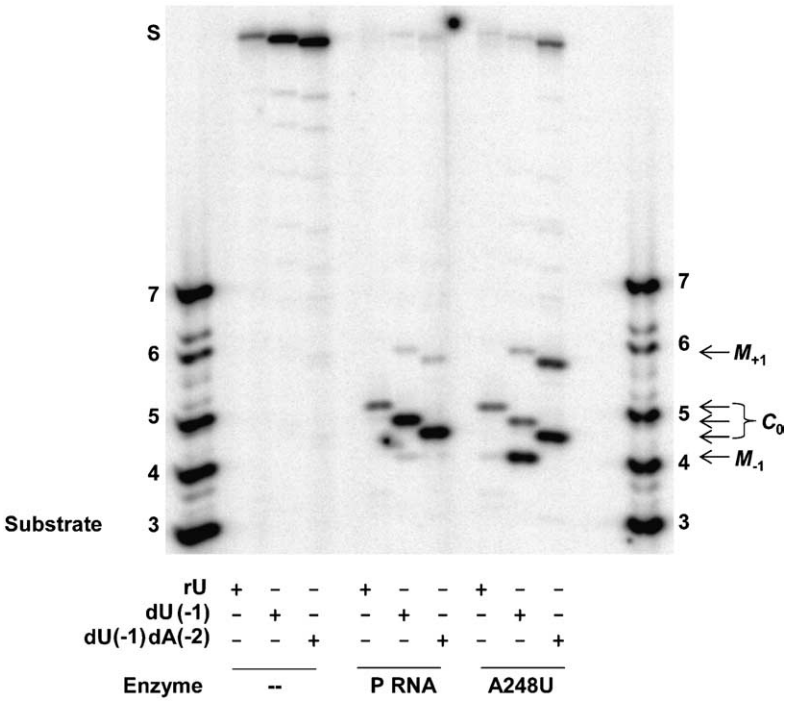

Figure 5. A 2′-deoxy modification at N(−2) blocks mis-cleavage at the M_{-1} site. Products of cleavage of the wild-type substrate (rU), N(−1)-deoxy substrate (dU(-1)) and N(−1), N(−2)-dideoxy substrate (dU(-1)dA(-2)) by either native or A248U RNase P RNA under standard reaction conditions and at pH 7.8 are shown. All substrates have the leader sequence AAAAU. Synthetic marker oligos indicating the mobility of three, four, five, six and seven nucleotide cleavage products are shown on the left and right. Mobility of uncleaved substrate is indicated (S). Cleavage at the C_0 site results in a five nucleotide product while cleavage at the M_{-1} site results in a four nucleotide product as indicated by arrows. Increased mobility of N(−1)-deoxy and N(−1),N(−2)-dideoxy products results from the ability of high-percentage polyacrylamide gels to resolve small oligonucleotides by backbone composition.

substitution at N(−2) reduces mis-cleavage of the dU(-1),dA(-2)-dideoxy substrate by the A248U mutant ribozyme to undetectable levels. This result indicates that the N(−2)-deoxy modification decreases $k_{1,app}$ for mis-cleavage at least 130-fold relative to $k_{1,app}$ for correct cleavage.† In addition, the N(−2)-deoxy modification increases the trace amount of mis-cleavage occurring one nucleotide 3′ of the correct cleavage site. Together, these results indicate that, in contrast to the results obtained with cleavage of a pre-tRNA^{Phe} substrate, the 2′-hydroxyl group of N(−2) is an important enzyme–substrate contact in the E–S_m complex for the model substrate employed here.

Energetic interdependence of the A248/N(−1) interaction and contacts to the 2′-hydroxyl group of N(−1) to binding and catalysis

As introduced above, mis-cleavage can formally arise from changes in the rates of cleavage for, and relative affinities of the E–S_c and E–S_m complexes. In addition, the catalytic and binding effects of disrupting contacts to the base and backbone of N(−1) position vary significantly in the literature. Therefore, to better determine how disruption of these contacts effects the process of cleavage site selection, we determined the effects of N(−1) mutation and 2′-deoxy substitution of the pre-tRNA^{Asp} substrate on binding affinity and the values of $k_{app,c}$ and $k_{app,m}$ for native and A248 mutant ribozymes (Table 2).

For catalysis, we observe that the combined effects of 2′-deoxy modification at N(−1) and disruption of the A248/N(−1) base-pairing interaction are synergistic. For example, with native P RNA a 2′-deoxy modification at N(−1) leads to a 31-fold decrease in the rate of cleavage at the correct cleavage site. However, in the context of a substrate with a U to A mutation at N(−1) the apparent effect of deoxy modification increases to 800-fold. Conversely, a U to A mutation at N(−1) has little effect on catalysis in the context of a substrate with ribose at N(−1), but has a significant, 40-fold effect in the presence of a 2′-deoxy modification. Similarly, with a U at N(−1), the kinetic defect of the A248U mutant at the correct site is increased from sixfold to 530-fold by N(−1)-deoxy modification. No mis-cleavage is observed for the U(−1), A(−1) and dU(-1) substrates; however, a substrate with a 2′-deoxy A at N(−1) is mis-cleaved to a small extent (F_c=0.8–0.9). Since some degree of mis-cleavage is observed with the dA(-1) substrate, quantitative comparison of apparent rates for N(−1)-ribo and N(−1)-deoxy substrates is problematic, since $k_{app,c}$ and $k_{app,m}$ contain equilibrium binding terms (see Materials and Methods). Nonetheless, the results clearly demonstrate that a significantly greater effect on the rate of catalysis is observed for a combined U to

† Given the relationship between F_c and the apparent second-order rates for cleavage at the C_0 and M_{-1} sites from equation (4), an F_c value of 0.13, corresponding to 87% mis-cleavage, indicates a 6.7-fold faster rate for cleavage at the M_{-1} site than at the C_0 site. Similarly, for F_c greater than 0.95, cleavage at M_{-1} must be at least 19-fold slower than cleavage at the C_0 site. Therefore, the increase of F_c from 0.13 to greater than 0.95 indicates a greater than 130-fold decrease in the rate of cleavage at the M_{-1} site relative to the rate of cleavage at the C_0 site.

Table 2. Effects of A248 and N(−1) mutations for N(−1)-deoxy substrates

Enzyme	Substrate	$k_{app,c}$ (min^{-1})[a]	$k_{app,c}/k_{wt}$	$k_{app,m}$ (min^{-1})[a]	$K_{d,obs}$ (nM)[b]	$k_{d,obs}/k_{d,wt}$
Native	U(−1) (native)	5.0±0.7[c]	–		1.8±0.5[c]	–
Native	A(−1)	3.2±0.1[c]	1.6		9.4±2.1[c]	5.2
A248U	U(−1)	0.8±0.1[c]	6.2		520±40[c]	290
A248U	A(−1)	2.2±0.5[c]	2.3		80±29[c]	45
Native	dU(-1)	0.16±0.05	31	$12\times10^{-3}\pm3\times10^{-3}$	640±50	350
Native	dA(-1)	$4\times10^{-3}\pm1\times10^{-3}$	1300	$5\times10^{-3}\pm1\times10^{-3}$	140±40	78
A248U	dU(-1)	$0.3\times10^{-3}\pm0.1\times10^{-3}$	17,000	$3\times10^{-3}\pm1\times10^{-3}$	1200±200[d]	670
A248U	dA(-1)	$0.9\times10^{-3}\pm0.2\times10^{-3}$	5500	$0.6\times10^{-3}\pm0.2\times10^{-3}$	460±170	260

[a] $k_{app,c}$ and $k_{app,m}$ values were determined from values of F_c and k_{obs} measured at saturating enzyme concentrations (see Materials and Methods). Indicated uncertainties represent the standard deviation of three or more independent trials.
[b] Values of $K_{d,obs}$ were obtained by gel mobility-shift assay at pH 6.0 and 25 mM Ca^{2+}. Indicated uncertainties represent the standard deviation of three or more trials.
[c] Values taken from Zahler *et al.*[15]
[d] It has been reported that $K_{d,obs}$ values greater than 1000 nM determined by gel mobility-shift may overestimate the actual $K_{d,value}$.[59]

A mutation and a 2′-deoxy modification than expected based on the effects of these individual modifications alone.

We also observe a strong correlation between the contributions to substrate binding by contacts to the backbone and nucleobase of N(−1), as assayed by gel mobility-shift experiments. As shown in Table 2, for the pre-tRNA^{Asp} substrate a 2′-deoxy modification at N(−1) results in a significant decrease in binding affinity, reflected in a 350-fold increase in the equilibrium dissociation constant ($K_{d,app}$). In contrast, when the N(−1) position is an A the deletion of the 2′-hydroxyl group at this position has only a ca 15-fold effect. Additionally, for N(−1)-deoxy substrates, we observe markedly reduced effects for disrupting the A248/N(−1) interaction. For example, an A to U mutation at position 248 results in a 290-fold effect with the native substrate. However, with a deoxy substrate, the largest effect, that of changing N(−1) from a U to an A in the substrate, results in only a two- to threefold change in $K_{d,obs}$. Furthermore, this mutation strengthens binding, rather than weakening, which is likely to be due to changes in ground state substrate structure rather than changes in ribozyme–substrate interactions. Together, these observations indicate that the A248/N(−1) interaction does not contribute strongly to the binding of N(−1) 2′-deoxy substrates.

Interplay between the contribution of base and backbone functional groups is also suggested by an analysis of the cleavage rate and binding affinity of these same substrates with the A248U mutant ribozyme. As reported previously, this mutation results in only a sixfold lower cleavage rate constant with the standard U(−1) substrate, but, remarkably this same mutant cleaves the dU(-1) substrate greater than 500-fold slower than the native P RNA. Our previous data as well as the results presented above show that mis-cleavage of substrates by A248U enzyme can be suppressed by changing N(−1) to A. Table 2 shows that suppression is due to a small increase in $k_{app,c}$ (threefold) but a larger decrease in $k_{app,m}$ (fivefold), changes which appear sufficient to tip the balance from essentially complete mis-cleavage to correct cleavage. Defining the basis for these interdependent effects is thus important for understanding how fidelity is maintained in substrates that lack a canonical set of interactions with the ribozyme.

Threshold effects on cleavage fidelity: mis-cleavage results from disruption of any subset of active site interactions

The data presented above support a model in which a 2′-deoxy modification at N(−1) results in a specific decrease in the rate of cleavage at the correct cleavage pathway. However, this pathway remains favorable relative to the mis-cleavage pathway, and the additional disruption of the A248/N(−1) is required to observe mis-cleavage. Thus, we hypothesize that, in this context, the two modifications act together to weaken the correct cleavage pathway beyond a specific "threshold", rendering the mis-cleavage pathway favorable. If this model is correct, any substrate mutation or modification that weakens binding, or slows catalysis specifically at the correct cleavage site, in combination with the disruption of the A248/N(−1) interaction, should also reveal mis-cleavage. Alternatively, given that both the contacts to the 2′-hydroxyl group of N(−1) and the A248/N(−1) interaction involve the same substrate nucleotide, the 2′-hydroxyl group of N(−1) may be unique in its relationship to the A248/N(−1) interaction. Also, it has been proposed that the 2′-hydroxyl group of N(−1) is recognized in a conformational change subsequent to the formation other ribozyme–substrate interactions.[15,17,35] In such a case, substrate modifications other than deletion of the 2′-hydroxyl group at N(−1) may show differential effects on enzyme specificity.

To better understand the interdependence of active site interactions with the pre-tRNA^{Asp} substrate, we examined the ability of substrate modifications to promote mis-cleavage when the A248/N(−1) interaction was also disrupted. For these experiments we employed substrates either

lacking the 3′-terminal CCA of the RCCA motif (ΔCCA), or bearing an R_P phosphorothioate modification at the correct cleavage site. These modifications were chosen because their effects on binding affinity and catalysis are relatively well characterized. As introduced above, interactions between the RCCA motif and the L15 internal bulge of RNase P RNA contribute to high affinity binding and cleavage site selection.[22,53,54] The R_P phosphorothioate modification at the correct cleavage site, like the N(−1)-deoxy modification, reduces the rate of chemistry at this site (k_c in Scheme 1) by several hundred-fold, but has little effect on fidelity.[19]

The results obtained with the native and A248U mutant ribozymes with ΔCCA substrates are shown in Figure 6(A). Like the N(−1) 2′-deoxy modification, the ΔCCA deletion alone does not engender mis-cleavage for the pre-tRNA^{Asp} substrate. However, when combined with enzyme or substrate mutations that disrupt the A248/N(−1) interaction, ΔCCA substrates show significant mis-cleavage at M_{-1}. In addition, the pattern of mis-cleavage we observe upon disruption of the interaction with the substrate 3′ end is similar to that observed for substrates with a 2′-deoxy modification at N(−1). For example, the combination of the A248U mutant ribozyme and pre-tRNA^{Asp} with a U at N(−1), but missing the 3′ CCA leads to significant mis-cleavage. This defect in fidelity is rescued by a compensatory mutation of U(−1) to A which restores the A248/N(−1) interaction by creating a U-A in place of the native A-U pairing interaction at N(−1).

We also tested the effects of combining modifications at the reactive phosphate group with the ΔCCA modification. As reported previously, N(−1) phosphorothioate modification at the pre-tRNA^{Asp}

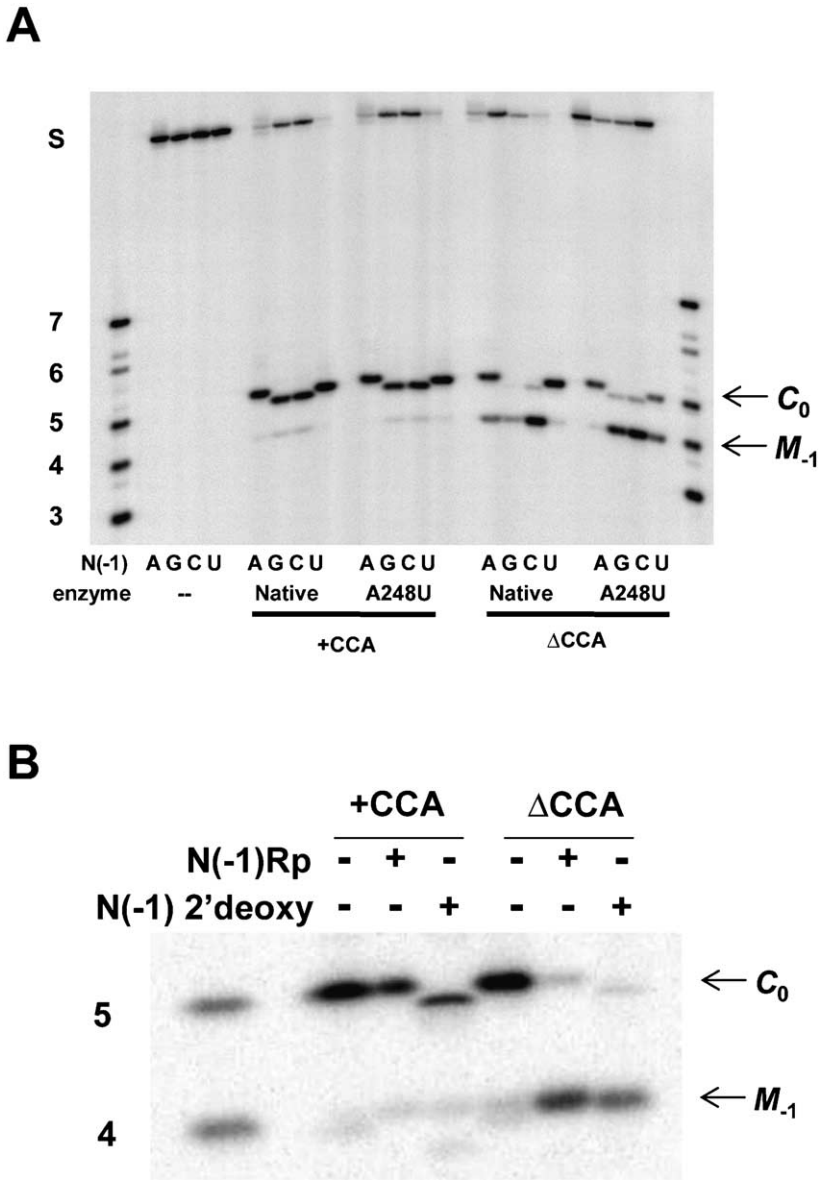

Figure 6. Cleavage site selection for ΔCCA substrates is dependent on interactions with N(−1). A, Cleavage site selection for substrates containing (+CCA) and lacking (ΔCCA) the last three nucleotides of the 3′-terminal RCCA motif. The identities of the nucleotide at position N(−1) are indicated. Reactions were carried out with annealed substrates under standard reaction conditions at pH 6.0. Markers showing the mobility of four, five, six and seven nucleotide cleavage products are shown on the left and right. Cleavage at the C_0 site results in a five nucleotide product while cleavage at the M_{-1} site results in a four nucleotide product as shown by arrows indicating the appropriate cleavage products. B, Cleavage site selection for substrates with ΔCCA, N(−1) deoxy, and N(−1) phosphorothioate modifications. Individual lanes show the cleavage products obtained for reactions of native RNase P RNA with substrates containing individual and combined R_P phosphorothioate substitution at the C_0 site (Rp), 2′-deoxy modification at N(−1) (Deoxy), and deletion of the CCA of the 3′-terminal RCCA motif (ΔCCA). Markers showing mobility of four and five nucleotide products are shown on the left. Cleavage at the C_0 site leads to a five nucleotide product and cleavage at the M_{-1} site leads to a four nucleotide product as indicated by arrows shown on the right. Reactions were carried out with annealed substrates at pH 6.0 under standard reaction conditions.

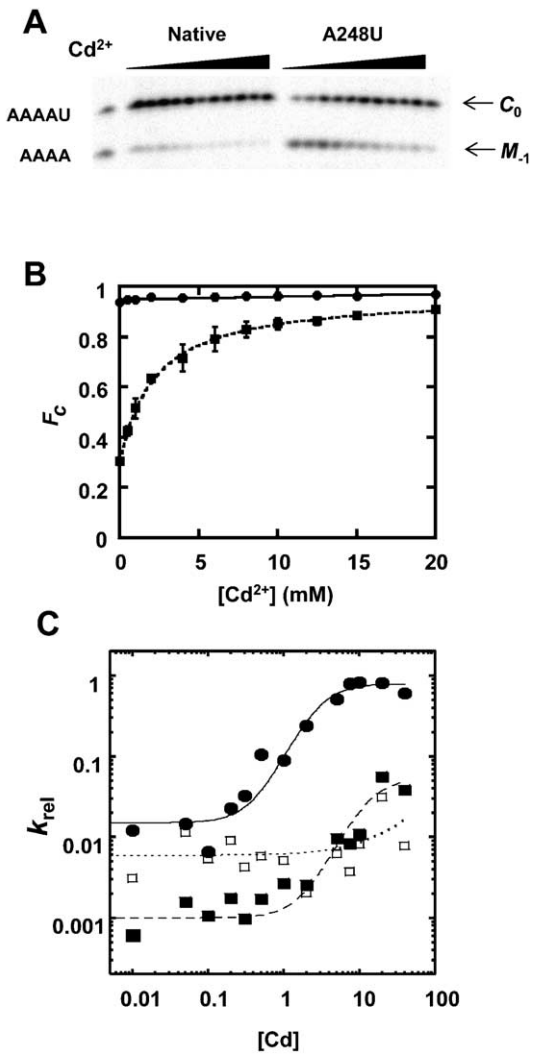

Figure 7. Cleavage site selection for Rp phosphorothioate containing substrates in the presence of Cd^{2+}. A, Cleavage products for ligated substrates containing an Rp phosphorothioate modification at the C_0 site. Markers on the left indicate the mobility of C_0 (AAAAU) and M_{-1} (AAAA) products. Reactions were carried out at pH 6.0 under standard reaction conditions with 10 mM Mg^{2+} and increasing concentrations of Cd^{2+}. B, Plot of F_c *versus* Cd^{2+} concentration for R_P phosphorothioate substrates cleaved by the native (circles) and A248U mutant (squares) ribozymes. Reaction conditions are as for A. Error bars indicate the standard deviation of three independent trials. Points where no error bars are visible have standard deviations of less than ± 0.01. C, Quantitative analysis of the effect of Cd^{2+} on $k_{app,c}$ and $k_{app,m}$. $k_{app,c}$ for Rp phosphorothioate containing substrates are plotted as k_{rel} (see Materials and Methods). Data show the effects of Cd^{2+} on the rate of cleavage at the C_0 site for the native P RNA (filled circles) and the A248U mutant ribzyme at the C_0 (filled squares) and M_{-1} sites (open squares). Data are fit to the non-linear form of the Hill equation (equation (9)).

cleavage site alone does not result in mis-cleavage by the native enzyme. However, combining the effect of this modification with deletion of the 3′ CCA sequence shifts cleavage almost entirely to the M_{-1} site (Figure 6B). The same result is observed with a 2′-deoxy modification at N(−1) where no mis-cleavage is observed with the single change, but cleavage occurs exclusively at M_{-1} when the 3′ CCA sequence is deleted as well. Thus, we conclude that mis-cleavage at the N(−1) site can arise from progressive disruption of interactions at the correct cleavage site and does not necessarily require the presence of new, non-native interactions that specifically stabilize E–S_m or enhance the rate of cleavage at the M_{-1} site.

Similar to the ΔCCA modification, reaction of a pre-$tRNA^{Asp}$ substrate containing an N(−1) phosphorothioate with the A248U mutant ribozyme results in significant cleavage at the M_{-1} site (Figure 7A). The rate defect engendered by R_P phosphorothioate modification at the correct cleavage site can be rescued by inclusion of the thiophillic metal ion Cd^{2+} in reactions.[19] In principle, this increase in the rate of cleavage at the C_0 site should, in turn, lead to an increase in F_c. As shown in Figure 7B, in the absence of Cd^{2+}, cleavage of the R_P phosphorothioate substrate by the A248U mutant ribozyme results in 70% cleavage at the M_{-1} site ($F_c \approx 0.3$). Addition of Cd^{2+} rescues this mis-cleavage up to an F_c of greater than 0.9 in a concentration-dependent manner. The Cd^{2+} dependence we observe for F_c can be fit to a single binding isotherm. However, because mis-cleavage results from competition between two pathways, and since it is possible that Cd^{2+} could alter the observed rates and binding affinities for both pathways, a quantitative assessment of specific metal binding affinity from these data is not possible. Nevertheless, these results are consistent with a mechanism in which phosphorothioate modification specifically decreases $k_{app,c}$ and the primary effect of Cd^{2+} is enhancing the rate of cleavage at the correct site *via* an interaction with the non-bridging sulfur atom at the reactive phosphate.

Additional insight into the cleavage and mis-cleavage pathways is provided by quantitative analysis of the Cd^{2+} dependence of $k_{app,c}$ and $k_{app,m}$ for the N(−1) phosphorothioate substrate. Figure 7C shows the Cd^{2+} dependence of $k_{app,c}$ for native and A248U P RNA, and $k_{app,m}$ for A248U P RNA. Note that the rate of catalysis at both sites will depend non-specifically on the overall metal ion concentration, and that Cd^{2+} may also have effects on the rate of cleavage of the substrate lacking a phosphorothioate modification. To control for non-specific effects of Cd^{2+} on the apparent rate of cleavage at the C_0 site, the values for $k_{app,c}$ in Figure 7 are expressed as relative rates compared to the rate of cleavage at the C_0 site of an unmodified substrate (k_{rel}; see Materials and Methods). This approach has been successfully used to gain insight into the number and affinity of the rescuing metal ions.[55–57]

The data shown in Figure 7C for native P RNA fit to a cooperative binding model with a Hill coefficient of 2 and $K_{1/2}^{Cd}$ value of ca 5 mM.

Importantly, the data for $k_{app,c}$ for the A248U mutant ribozyme also fit to a cooperative binding model with only small changes in the cooperativity and affinity parameters. In contrast, the magnitude of $k_{app,m}$ is essentially unaffected by Cd^{2+} and remains constant over the range of concentrations tested. Because the dependence of $k_{app,c}$ on Cd^{2+} concentration are similar for P RNA and for the A248U mutant, we infer that under these conditions the rate-limiting step for the correct cleavage pathway with the A248U mutant is the same as with the native ribozyme. A simple explanation for this behavior is that the addition of Cd^{2+} rescues mis-cleavage by specifically enhancing the rate of cleavage at the C_0 site, with little effect on cleavage at the M_{-1} site, consistent with the insensitivity of $k_{app,m}$ with respect to Cd^{2+} concentration. Additionally, while the values of n and $K_{1/2}^{Cd}$ for the native and A248U mutant P RNAs cannot be compared quantitatively due to the complexities introduced by mis-cleavage, their similarity suggests that disruption of the A248/N(−1) interaction has little effect on the apparent affinity of the rescuing Cd ions. This observation supports the conclusion from Mg^{2+} titration studies (see above; Figure 3) that although the A248/N(−1) interaction contributes to specificity by enhancing the rate of chemistry at the adjacent phosphodiester bond, it does not have an apparent influence on the affinity of metal ions required for catalysis.

Discussion

The results presented here are consistent with a strong network of active site interactions that position the appropriate phosphodiester bond in the P RNA active site. For example, an N(−1) 2′-deoxy modification reduces both binding affinity and catalysis dramatically, yet these effects together are not sufficient to render the M_{-1} site favorable. However, combining any two of the modifications or mutations tested here causes significant levels of mis-cleavage. Thus, for an "optimal" substrate, such as pre-$tRNA^{Asp}$, which appears to contain all of the known RNase P recognition elements, the correct cleavage site is essentially over-defined. For such substrates, the preference for the C_0 site over the M_{-1} site is such that cleavage site selection does not hinge upon any one interaction. Instead, and as might be expected for an enzyme that processes structurally diverse substrates, a number of different subsets of potential interactions are sufficient to ensure correct cleavage. Mis-cleavage is thus only observed after the correct enzyme substrate complex ($E–S_c$) is destabilized beyond a certain threshold. This general scheme predicts that other substrates that lack a canonical RNase P recognition structure will be more sensitive to effects of functional group modifications on fidelity.

In a qualitative sense, analysis of the effect of functional group modifications on the site and amount of substrate mis-cleavage is a facile system for examination of the structural features of the correct ($E–S_c$) and mis-cleavage ($E–S_m$) complexes. As shown in Figure 8 the data presented here are consistent with previous analyses showing formation of an interaction between position 248 in the J5/15 element of the ribozyme and nucleotide N(−2) that favors mis-cleavage.[15] Additionally, we find that the 2′-hydroxyl group adjacent to the cleavage site is also recognized in the mis-cleavage complex as evidenced by the observation that a 2′-deoxy substitution here results in a "rescue" of cleavage specificity. It is unclear whether the mis-cleavage complex retains or has altered interactions with the 3′ RCCA sequence. Weakening this interaction results in formation of $E–S_m$ and resultant mis-cleavage when interactions with the 2′-hydroxyl and non-bridging phosphate oxygen atoms at C_0 are disrupted. These results are consistent with previous studies demonstrating that these interactions promote the formation of $E–S_c$.

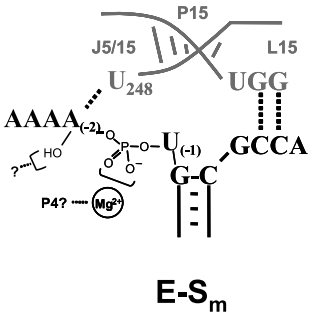

Figure 8. Schematic representation of the proposed structure of an $E–S_m$ complex. The pre-tRNA cleavage site is shown in black with bold letters representing proposed recognition elements; P RNA sequences are shown in gray. Dotted lines indicate proposed hydrogen bonding interactions. Active site interactions with the 2′-hydroxyl group and non-bridging oxygen atoms at the reactive phosphate group are denoted by brackets.

It is assumed that the catalytic mechanism is the same in the correct and mis-cleavage complexes (Figure 8), including the interactions between active site metal ions and the reactive phosphate. The finding that F_c is relatively insensitive to Mg^{2+} concentrations supports this assumption. However, quantitative analyses of the Mg^{2+} titration data suggest that there are some important differences in the metal ion dependence of the correct and mis-cleavage pathways. Notably the apparent Mg^{2+} dependence of mis-cleavage is less cooperative and has a weaker apparent affinity. One possibility is that there is an intrinsic difference in number and affinity of active site metal ions in the $E–S_m$ complex. It is also possible that the two pathways have different rate-limiting steps, and that the concentration dependence of the catalytic step is masked by the requirement for metal ion binding for other aspects of the reaction such as binding. The interpretation that apparent differences in

metal ion sensitivity are due to differences in rate limiting step is also supported by the lesser degree of pH sensitivity of the rate of cleavage at M_{-1} relative to C_0.

The results presented here also have important implications for understanding the role of the 2′-hydroxyl of N(−1) in RNase P catalysis. It was recently proposed that the 2′-hydroxyl of N(−1) is an outer-sphere ligand for a catalytically important divalent metal ion.[25] In addition to data from metal ion titrations, this conclusion is supported by the ability of increased pH to rescue the mis-cleavage phenotype of a 2′-amino modification at N(−1). It was suggested that this pH dependent rescue was due to the deprotonation of the 2′ amine group, allowing it to participate in metal ion binding. However, our results demonstrate clearly that a pH-dependent rescue of mis-cleavage can and does arise due to differences in the kinetic mechanism for cleavage at the C_0 and M_{-1} sites in the absence of an introduced titratable functional group. Furthermore, we observe pH-dependent rescue of mis-cleavage for an N(−1)-deoxy substrate over the same pH range as that reported for the 2′-amine substrate modification. Thus, while the 2′-hydroxyl group of N(−1) may indeed function as a metal ion ligand, the ability of increased pH to rescue mis-cleavage caused by 2′-amino substitution may not necessarily reflect such an interaction.

Additional information concerning the process of recognition of the correct cleavage site is provided by kinetic and thermodynamic analysis of the effects of mutations which disrupt interactions with the nucleobase and 2′-hydroxyl group of N(−1). In the presence of an N(−1) deoxy modification, the apparent catalytic effects of disrupting the A248/N(−1) interaction are orders of magnitude larger than the effects of the same mutations in the absence of the N(−1) deoxy modification (see Table 2). Conversely, the catalytic effects of the N(−1)-deoxy modification are significantly larger in the presence of mutations at A248 or N(−1). In contrast, we observe a significantly less than additive effect for simultaneous A248/N(−1) disruption and N(−1)-deoxy modification on substrate binding (see Table 2). For unmodified substrates, mutations that disrupt the A248/N(−1) interaction have significant affects on substrate binding affinity. However, in the presence of the N(−1)-deoxy modification, the substrate binding effects of A248/N(−1) disruption are greatly suppressed. Additionally, the range of observed $K_{d,app}$ values for mutations at A248 and N(−1) is reduced by two orders of magnitude in the presence of the N(−1)-deoxy modification. The 2′-deoxy modification at N(−1) also changes the pattern of favorable and unfavorable mutations at these positions. Thus, the presence of a 2′-deoxy modification enhances effects of N(−1) mutation on catalysis, but suppresses effects on ground state binding.

For unmodified substrates, the pattern of substrate binding effects is consistent with *cis* Watson–Crick/Watson–Crick base-pairing between A248 and N(−1). For example, the A248U mutation exhibits a large binding defect which can be partially rescued by mutating N(−1) from U to A, and the binding defect engendered by an A248C mutation can be completely rescued by a U to G mutation at N(−1). This suggests that the E–S_c complex in which the ribozyme/N(−1) interaction has formed is the predominant form of the enzyme–substrate complex. In the presence of the N(−1)-deoxy modification, however, this pattern changes. For example, a U to A mutation at N(−1) enhances rather than weakens binding to the native enzyme. While this is not consistent with the E–S_c complex being the predominant form of the enzyme–substrate complex, it is also not consistent with what we would expect for the E–S_m complex. For example, if the E–S_m is the predominant form, we would expect that the A248U mutant would bind the dU(-1) substrate tighter than the native enzyme, rather than slightly weaker, as we observe. Thus, the observed binding effects are not consistent with either the E–S_c or the E–S_m complex being the predominant ground state complex for N(−1)-deoxy substrates.

Instead, these results are consistent with mechanisms in which the A248/N(−1) interaction is not formed upon initial substrate binding, in a manner similar to that proposed for recognition of the 2′-hydroxyl of N(−1).[35,36] According to this mechanism a complex (E–S) results from initial binding in which only a subset of active site interactions have formed, exclusive of the base and backbone of N(−1). Subsequently, interactions with the nucleotide upstream of the eventual cleavage site form and the complex (E–S*) becomes committed to catalysis. The equilibrium for formation of the E–S* complex from E–S is likely to be highly favored; however, N(−1)-deoxy modification and disruption of the A248/N(−1) interaction may both be sufficient to destabilize the E–S* complex relative to the initial binding complex (E–S). Either modification then would result in an observed binding defect and E–S would then be the predominant form of the enzyme–substrate complex. Thus, disruption of either the base or backbone contact to N(−1) destabilizes E–S* such that E–S establishes a new ground state. Further disruption of N(−1) interactions would then destabilize the transition state, but not the ground state and large effects on the rate of catalysis are observed.

Such multi-step mechanisms for substrate recognition are not unexpected given the conformational changes that have been characterized for other ribozymes. For example, it is well-established that substrate binding by the L21Sca version of the group I intron ribozyme involves a docking step after binding which positions the correct phosphodiester bond in the ribozyme active site.[64–67] This docking step depends on interactions with 2′ hydroxyl groups in the helix formed by base-pariing between the oligonucleotide substrate and

the ribozyme. Modification of these 2′ hydroxyl groups can result in loss of fidelity due to formation of alternative interactions with other hydroxyl groups in the substrate stem.[66] Such as situation is similar to RNase P as 2′ deoxy substitution at the cleavage site leads to mis-cleavage. Similarly, phosphorothioate modifications at the reactive phosphate group within mutant substrates can also lead to loss of fidelity in the group I intron due to large changes in the relative rates of cleavage at the correct and incorrect sites.[65]

The threshold model outlined above provides an explanation for apparent discrepancies in the literature regarding the effects of N(−1)-deoxy modification. Previous studies examining the role of the 2′-hydroxyl group of N(−1) report a wide range of values for the kinetic defects engendered by deoxy modification.[25,26,35,36] In addition, there is disagreement in the literature with regard to the effects of N(−1)-deoxy modification on substrate binding. Some studies report that the N(−1)-deoxy modification has no effect on substrate binding, while others show large binding defects. The results presented here establish that at least one factor that contributes to this range of apparent effects is the presence or absence of the A248/N(−1) interaction. Our results reproduce situations in which the 2′-deoxy modification at N(−1) has both substantial and negligible effects on substrate binding by simply varying A248 and N(−1). Furthermore, we observe that maximal effects for an N(−1) 2′-deoxy modification with regard to kinetics and substrate binding are observed for enzyme–substrate combinations in which the A248/N(−1) interaction is present. Previous studies have employed substrates with different nucleobases at N(−1) when examining the importance of this functional group resulting in different reported magnitudes for the contribution of this functional group to catalysis. Given the range of effects observed for this 2′-deoxy modification for N(−1) mutant substrates, future experiments that examine the effects of 2′-hydroxyl modification at N(−1) must take into account the context in which this interaction occurs, including the identity of the nucleotide at N(−1). Nevertheless, making structural interpretations from kinetic and thermodynamic data is challenging, and direct physical tests for the occurrence and importance of conformational changes in the RNase P reaction will be necessary.

Materials and Methods

General methods

Enzyme RNAs were produced by run-off transcription according to standard protocols.[40] Substrates used for kinetic and gel mobility-shift assays were produced by ligating two synthetic RNA oligonucleotides[62] according to published protocols.[63] For these ligations, a 5′ radiolabeled oligonucleotide comprising pre-tRNA^{Asp} nucleotides −5 through +9 (5′LS-RNA) was ligated to an oligonucleotide comprising the remainder of the pre-tRNA substrate. Oligonucleotides were purchased from Dharmacon Inc, and gel-purified prior to use. The 5′LS-RNA oligonucleotide containing an R_P phosphorothioate modification at the cleavage site was purified by reverse-phase high-pressure liquid chromatography.[60,64]

For experiments examining cleavage site selection, we took advantage of the ability of the oligonucleotides described above to form a substrate stabilized by the 7 bp of the pre-tRNA acceptor stem in the absence of ligation.[15,61,65] Such annealed substrates are cleaved at the correct site, show quantitatively the same cleavage site selection as ligated substrates and have identical single-turnover reaction rates as ligated substrates (N.H.Z. and M.E.H., unpublished results). Reactions with annealed substrates, unless otherwise specified, were carried out under standard reaction conditions, and contained 4 nM radiolabeled 5′ oligonucleotides, 100 nM 3′ oligonucleotides and 1 μM RNase P RNA.

Standard reaction conditions were 1 M ammonium acetate and 25 mM $MgCl_2$. pH buffers varied depending on the desired pH of the reaction. Reactions at pH 5.5 contained a final concentration of 20 mM Mes; pH 6.0 and 7.0 reactions included 20 mM Pipes; and pH 7.8 reactions contained 20 mM Tris. The pH of all buffers was adjusted at 37 °C. Reactions in which conditions differed from the standard, such as Cd^{2+} and Mg^{2+} titrations are noted in the Figure legends.

Prior to reaction, enzymes and substrates were renatured separately by heating to 95 °C for three minutes in buffer lacking divalent metal ions. Mixtures were subsequently cooled to 37 °C and allowed to incubate for ten minutes prior to addition of divalent metal ion. Mixtures were then allowed to incubate for at least 30 minutes prior to initiating reactions by mixing enzyme and substrate. Renaturations and subsequent reactions were carried out in a Hybaid Omn-E thermocycler with a heated lid to ensure constant temperature and minimize evaporation. For reactions that were allowed to proceed overnight or longer, reaction mixtures were overlaid with mineral oil to prevent evaporation. Reactions were stopped by mixing with gel-loading buffer containing 100 mM EDTA in formamide, and products were separated by denaturing 22.5% (w/v) PAGE.

Kinetic and thermodynamic analyses

For single-turnover kinetic experiments, reactions were carried out with 4 nM final concentration of ligated substrate and two enzyme concentrations, generally 5 μM and 10 μM. Enzyme concentrations were determined to be saturating if the observed change in rate upon doubling enzyme concentration was less than 10%. Values of $K_{d,app}$ were measured by gel mobility-shift experiments at pH 6.0 and with 25 mM $CaCl_2$, as described.[58]

For N(−1)-deoxy substrates that show significant cleavage at the M_{-1} site, we employed an analysis based on the model shown in Scheme 1.[35,36,45,46] In this model, the increase in C_0 and M_{-1} cleavage products over time are described by equations (1) and (2), respectively:

$$P_c = F_c(1 - e^{-k_{obs}t}) \quad (1)$$

$$P_{M-1} = (1 - F_c)(1 - e^{-k_{obs}t}) \quad (2)$$

In equations (1) and (2), P_c and P_{M-1} are the fractions of substrate that have been cleaved at the C_0 and M_{-1} sites, respectively; F_c is the fraction of substrate cleaved at the C_0 site at infinite time; and k_{obs} is the observed rate of the

reaction. For cleavage at the C_0 and M_{-1} sites at saturating enzyme concentrations, k_{obs} is described by equation (3):

$$k_{obs} = \frac{K_c k_c + K_m k_m}{K_c + K_m} \quad (3)$$

where K_c, K_m, k_c, and k_m are equilibrium substrate association and rate constants shown in Scheme 1. Finally, for this model, if cleavage is rate limiting, F_c is defined according to equation (4):

$$F_c = \frac{K_c k_c}{K_c k_c + K_m k_m} = \frac{k_{1c,app}}{k_{1c,app} + k_{1m,app}} \quad (4)$$

where $k_{1c,app}$ and $k_{1m,app}$ are the apparent second-order rate constants for cleavage of substrate at the C_0 and M_{-1} sites, respectively.

As noted previously for a mechanism involving three cleavage sites, given values for F_c and k_{obs}, it is possible to calculate apparent first-order rate constants for cleavage at the C_0 and M_{-1} sites,[35] as shown in equations (5) and (6):

$$k_{app,c} = k_{obs} F_c = k_c \left(1 + \frac{K_m}{K_c}\right)^{-1} \quad (5)$$

$$k_{app,m} = k_{obs}(1 - F_c) = k_m \left(1 + \frac{K_c}{K_m}\right)^{-1} \quad (6)$$

In equations (5) and (6), $k_{app,c}$ and $k_{app,m}$ are the apparent first-order rate constants for cleavage at the C_0 and M_{-1} sites, respectively; k_c and k_m are rate constants shown in Scheme 1; and K_c and K_m are equilibrium constants also defined in Scheme 1.

Mg^{2+} titration experiments

Mg^{2+} titration experiments were carried out at pH 8, and under standard reaction conditions. Final enzyme concentrations in these experiments were 1 μM, a concentration low enough to avoid impacting the concentration of free Mg^{2+} in solution.[39] As shown above, cleavage site selection is determined by the apparent second-order rate constants for cleavage at the C_0 and M_{-1} sites, both of which are cooperatively dependent upon Mg^{2+} concentration in RNase P. Thus, cleavage at both the C_0 and M_{-1} sites is expected to behave according to the relationship in equation (7):

$$k_{1,app} = \frac{k_{1,max}[Mg^{2+}]^n}{[Mg^{2+}]^n + (K_{1/2}^{Mg})^n} \quad (7)$$

where $k_{1,app}$ is the apparent second-order rate constant, $k_{1,max}$ is the maximal rate constant at saturating Mg^{2+} concentrations, $K_{1/2}^{Mg}$ is the Mg^{2+} concentration required to achieve half the maximal rate, and n is the Hill coefficient. Given this cooperative dependence and the relationship in equation (4), the Mg^{2+} concentration dependence of F_c is described by equation (8):

$$F_c = \left[1 + \left(\frac{k_{m,max}}{k_{c,max}}\right)([Mg^{2+}]^{(n_m - n_c)})\left(\frac{(K_{1/2}^{Mg})^{n_c} + [Mg^{2+}]^{n_c}}{(K_{1/2}^{Mg})^{n_m} + [Mg^{2+}]^{n_m}}\right)\right]^{-1} \quad (8)$$

where $k_{c,max}$ and $k_{m,max}$ are the rates of cleavage at the correct and mis-cleavage sites at saturating Mg^{2+} concentrations; n_c and n_m are the Hill coefficients for correct cleavage and mis-cleavage; and $K_{1/2\,c}^{Mg}$ and $K_{1/2\,m}^{Mg}$ are the Mg^{2+} concentrations required to achieve half maximal cleavage rates at the C_0 and M_{-1} sites. It is important to note that in fitting F_c data, while the ratio of $k_{m,max}$ to $k_{c,max}$ can be determined, these two variables are not independent; however, the remaining variables can be determined unambiguously.

Quantitative thiophilic metal ion rescue experiments

Measurement of the apparent Cd^{2+} affinity for a sulfur atom substituted at the *pro*-R_P position of the scissile phosphate group was determined from the concentration dependence of the ability of Cd^{2+} to alleviate inhibition of the reaction due to the sulfur substitution essentially as described by Shan & Herschlag for the group I intron.[55,56] The pseudo-first-order reaction rate constants ($k_{app,c}$ and $k_{app,m}$) for substrates with an Rp phosphorothioate at the correct cleavage site were determined at a series of Cd^{2+} concentrations, as described above. To control for non-specific effects on ribozyme structure due to changes in divalent ion concentration the relative reaction rate, k_{rel}, was calculated from the ratio of the observed reaction rates of pre-tRNA substrates with and without the sulfur substitution (e.g. $k_{rel} = k_{aap,c}^{s}/k_{app,c}$). Plots of k_{rel} *versus* added Cd^{2+} concentration ($[Cd^{2+}]$) were fit with a non-linear form of the Hill equation for cooperative binding:

$$k_{rel} = \frac{k_{max}[Cd^{2+}]^n}{(K_{1/2}^{Cd})^n + [Cd^{2+}]^n} \quad (9)$$

where n is the Hill coefficient and $K_{1/2}^{Cd}$ represents the Cd^{2+} concentration required to attain half the maximal rate.

Acknowledgements

These studies were supported by NIH grant 56742 (to M.E.H.). N.H.Z. was supported, in part, by NIH training grant GM008056. We are grateful to Dr Tao Pan for advice on quantitative interpretation of substrate mis-cleavage and especially to Dr Frank Campbell for insightful comments on the manuscript.

References

1. Rupert, P. B. & Ferre-D'Amare, A. R. (2001). Crystal structure of a hairpin ribozyme–inhibitor complex with implications for catalysis. *Nature*, **410**, 780–786.
2. Pley, H. W., Flaherty, K. M. & McKay, D. B. (1994). Three-dimensional structure of a hammerhead ribozyme. *Nature*, **372**, 68–74.
3. Ferre-D'Amare, A. R., Zhou, K. & Doudna, J. A. (1998). Crystal structure of a hepatitis delta virus ribozyme. *Nature*, **395**, 567–574.
4. Kraut, D. A., Carroll, K. S. & Herschlag, D. (2003). Challenges in enzyme mechanism and energetics. *Annu. Rev. Biochem.* **72**, 517–571.
5. Morrissey, J. P. & Tollervey, D. (1995). Birth of the snoRNPs: the evolution of RNase MRP and the eukaryotic pre-rRNA-processing system. *Trends Biochem. Sci.* **20**, 78–82.

6. Frank, D. N. & Pace, N. R. (1998). Ribonuclease P: unity and diversity in a tRNA processing ribozyme. *Annu. Rev. Biochem.* **67**, 153–180.
7. Caprara, M. G. & Nilsen, T. W. (2000). RNA: versatility in form and function. *Nature Struct. Biol.* **7**, 831–833.
8. Guerrier-Takada, C. & Altman, S. (1984). Catalytic activity of an RNA molecule prepared by transcription *in vitro*. *Science*, **223**, 285–286.
9. Kurz, J. C., Niranjanakumari, S. & Fierke, C. A. (1998). Protein component of *Bacillus subtilis* RNase P specifically enhances the affinity for precursor-tRNAAsp. *Biochemistry*, **37**, 2393–2400.
10. Niranjanakumari, S., Stams, T., Crary, S. M., Christianson, D. W. & Fierke, C. A. (1998). Protein component of the ribozyme ribonuclease P alters substrate recognition by directly contacting precursor tRNA. *Proc. Natl Acad. Sci. USA*, **95**, 15212–15217.
11. Crary, S. M., Niranjanakumari, S. & Fierke, C. A. (1998). The protein component of *Bacillus subtilis* ribonuclease P increases catalytic efficiency by enhancing interactions with the 5′ leader sequence of pre-tRNAAsp. *Biochemistry*, **37**, 9409–9416.
12. Christian, E. L., Zahler, N. H., Kaye, N. M. & Harris, M. E. (2002). Analysis of substrate recognition by the ribonucleoprotein endonuclease RNase P. *Methods*, **28**, 307–322.
13. Kurz, J. C. & Fierke, C. A. (2000). Ribonuclease P: a ribonucleoprotein enzyme. *Curr. Opin. Chem. Biol.* **4**, 553–558.
14. Harris, M. E. & Christian, E. L. (2003). Recent insights into the structure and function of the ribonucleoprotein enzyme ribonuclease P. *Curr. Opin. Struct. Biol.* **13**, 325–333.
15. Zahler, N. H., Christian, E. L. & Harris, M. E. (2003). Recognition of the 5′ leader of pre-tRNA substrates by the active site of ribonuclease P. *RNA*, **9**, 734–745.
16. Lowe, T. M. & Eddy, S. R. (1997). tRNAscan-SE: a program for improved detection of transfer RNA genes in genomic sequence. *Nucl. Acids Res.* **25**, 955–964.
17. Brannvall, M., Fredrik Pettersson, B. M. & Kirsebom, L. A. (2002). The residue immediately upstream of the RNase P cleavage site is a positive determinant. *Biochimie*, **84**, 693–703.
18. Kirsebom, L. A. (2002). RNase P RNA-mediated catalysis. *Biochem. Soc. Trans.* **30**, 1153–1158.
19. Warnecke, J. M., Furste, J. P., Hardt, W. D., Erdmann, V. A. & Hartmann, R. K. (1996). Ribonuclease P (RNase P) RNA is converted to a Cd(2+)-ribozyme by a single Rp-phosphorothioate modification in the precursor tRNA at the RNase P cleavage site. *Proc. Natl Acad. Sci. USA*, **93**, 8924–8928.
20. Warnecke, J. M., Held, R., Busch, S. & Hartmann, R. K. (1999). Role of metal ions in the hydrolysis reaction catalyzed by RNase P RNA from *Bacillus subtilis*. *J. Mol. Biol.* **290**, 433–445.
21. Chen, Y., Li, X. & Gegenheimer, P. (1997). Ribonuclease P catalysis requires Mg^{2+} coordinated to the pro-RP oxygen of the scissile bond. *Biochemistry*, **36**, 2425–2438.
22. Kirsebom, L. A. & Svard, S. G. (1994). Base pairing between *Escherichia coli* RNase P RNA and its substrate. *EMBO J.* **13**, 4870–4876.
23. Brannvall, M. & Kirsebom, L. A. (1999). Manganese ions induce miscleavage in the *Escherichia coli* RNase P RNA- catalyzed reaction. *J. Mol. Biol.* **292**, 53–63.
24. Brannvall, M. & Kirsebom, L. A. (2001). Metal ion cooperativity in ribozyme cleavage of RNA. *Proc. Natl Acad. Sci. USA*, **98**, 12943–12947.
25. Persson, T., Cuzic, S. & Hartmann, R. K. (2003). Catalysis by RNase P RNA: unique features and unprecedented active site plasticity. *J. Biol. Chem.* **278**, 43394–43401.
26. Smith, D. & Pace, N. R. (1993). Multiple magnesium ions in the ribonuclease P reaction mechanism. *Biochemistry*, **32**, 5273–5281.
27. Perreault, J. P. & Altman, S. (1992). Important 2′-hydroxyl groups in model substrates for M1 RNA, the catalytic RNA subunit of RNase P from *Escherichia coli*. *J. Mol. Biol.* **226**, 399–409.
28. Loria, A., Niranjanakumari, S., Fierke, C. A. & Pan, T. (1998). Recognition of a pre-tRNA substrate by the *Bacillus subtilis* RNase P holoenzyme. *Biochemistry*, **37**, 15466–15473.
29. Bokinsky, G., Rueda, D., Misra, V. K., Rhodes, M. M., Gordus, A., Babcock, H. P. *et al*. (2003). Single-molecule transition-state analysis of RNA folding. *Proc. Natl Acad. Sci. USA*, **100**, 9302–9307.
30. Walter, N. G. (2001). Structural dynamics of catalytic RNA highlighted by fluorescence resonance energy transfer. *Methods*, **25**, 19–30.
31. Lafontaine, D. A., Norman, D. G. & Lilley, D. M. (2001). Structure, folding and activity of the VS ribozyme: importance of the 2-3-6 helical junction. *EMBO J.* **20**, 1415–1424.
32. Bevilacqua, P. C., Li, Y. & Turner, D. H. (1994). Fluorescence-detected stopped flow with a pyrene labeled substrate reveals that guanosine facilitates docking of the 5′ cleavage site into a high free energy binding mode in the *Tetrahymena* ribozyme. *Biochemistry*, **33**, 11340–11348.
33. Pomeranz Krummel, D. A., Kent, O., MacMillan, A. M. & Altman, S. (2000). Evidence for helical unwinding of an RNA substrate by the RNA enzyme RNase P: use of an interstrand disulfide crosslink in substrate. *J. Mol. Biol.* **295**, 1113–1118.
34. Pomeranz Krummel, D. A. & Altman, S. (1999). Multiple binding modes of substrate to the catalytic RNA subunit of RNase P from *Escherichia coli*. *RNA*, **5**, 1021–1033.
35. Loria, A. & Pan, T. (1998). Recognition of the 5′ leader and the acceptor stem of a pre-tRNA substrate by the ribozyme from *Bacillus subtilis* RNase P. *Biochemistry*, **37**, 10126–10133.
36. Loria, A. & Pan, T. (1999). The cleavage step of ribonuclease P catalysis is determined by ribozyme–substrate interactions both distal and proximal to the cleavage site. *Biochemistry*, **38**, 8612–8620.
37. Beebe, J. A. & Fierke, C. A. (1994). A kinetic mechanism for cleavage of precursor tRNA(Asp) catalyzed by the RNA component of *Bacillus subtilis* ribonuclease P. *Biochemistry*, **33**, 10294–10304.
38. Beebe, J. A., Kurz, J. C. & Fierke, C. A. (1996). Magnesium ions are required by *Bacillus subtilis* ribonuclease P RNA for both binding and cleaving precursor tRNAAsp. *Biochemistry*, **35**, 10493–104505.
39. Kurz, J. C. & Fierke, C. A. (2002). The affinity of magnesium binding sites in the *Bacillus subtilis* RNase P×pre-tRNA complex is enhanced by the protein subunit. *Biochemistry*, **41**, 9545–9558.
40. Siew, D., Zahler, N. H., Cassano, A. G., Strobel, S. A. & Harris, M. E. (1999). Identification of adenosine functional groups involved in substrate binding by the ribonuclease P ribozyme. *Biochemistry*, **38**, 1873–1883.

41. Christian, E. L. & Harris, M. E. (1999). The track of the pre-tRNA 5′ leader in the ribonuclease P ribozyme–substrate complex. *Biochemistry*, **38**, 12629–12638.
42. Christian, E. L., McPheeters, D. S. & Harris, M. E. (1998). Identification of individual nucleotides in the bacterial ribonuclease P ribozyme adjacent to the pre-tRNA cleavage site by short-range photo-cross-linking. *Biochemistry*, **37**, 17618–17628.
43. Chen, J. L., Nolan, J. M., Harris, M. E. & Pace, N. R. (1998). Comparative photocross-linking analysis of the tertiary structures of *Escherichia coli* and *Bacillus subtilis* RNase P RNAs. *EMBO J.* **17**, 1515–1525.
44. Harris, M. E., Nolan, J. M., Malhotra, A., Brown, J. W., Harvey, S. C. & Pace, N. R. (1994). Use of photoaffinity crosslinking and molecular modeling to analyze the global architecture of ribonuclease P RNA. *EMBO J.* **13**, 3953–3963.
45. Fersht, A. (1998). *Structure and Mechanism in Protein Science*, Freemand, New York.
46. Jencks, W. P. (1987). *Catalysis in Chemistry and Enzymology*, Dover, New York.
47. Smith, D., Burgin, A. B., Haas, E. S. & Pace, N. R. (1992). Influence of metal ions on the ribonuclease P reaction. Distinguishing substrate binding from catalysis. *J. Biol. Chem.* **267**, 2429–2436.
48. Kaye, N. M., Zahler, N. H., Christian, E. L. & Harris, M. E. (2002). Conservation of helical structure contributes to functional metal ion interactions in the catalytic domain of ribonuclease P RNA. *J. Mol. Biol.* **324**, 429–442.
49. Guerrier-Takada, C., Haydock, K., Allen, L. & Altman, S. (1986). Metal ion requirements and other aspects of the reaction catalyzed by M1 RNA, the RNA subunit of ribonuclease P from *Escherichia coli*. *Biochemistry*, **25**, 1509–1515.
50. Christian, E. L., Kaye, N. M. & Harris, M. E. (2002). Evidence for a polynuclear metal ion binding site in the catalytic domain of ribonuclease P RNA. *EMBO J.* **21**, 2253–2262.
51. Kirby, A. J. & Younas, M. (1970). The reactivity of phosphate esters. Reactions of diesters with nucleophiles. *J. Chem. Soc. B*, 1165–1172.
52. Cassano, A. G., Anderson, V. E. & Harris, M. E. (2002). Evidence for direct attack by hydroxide in phosphodiester hydrolysis. *J. Am. Chem. Soc.* **124**, 10964–10965.
53. Tallsjo, A., Kufel, J. & Kirsebom, L. A. (1996). Interaction between *Escherichia coli* RNase P RNA and the discriminator base results in slow product release. *RNA*, **2**, 299–307.
54. Brannvall, M., Mattsson, J. G., Svard, S. G. & Kirsebom, L. A. (1998). RNase P RNA structure and cleavage reflect the primary structure of tRNA genes. *J. Mol. Biol.* **283**, 771–783.
55. Shan, S., Kravchuk, A. V., Piccirilli, J. A. & Herschlag, D. (2001). Defining the catalytic metal ion interactions in the *Tetrahymena* ribozyme reaction. *Biochemistry*, **40**, 5161–5171.
56. Shan, S., Yoshida, A., Sun, S., Piccirilli, J. A. & Herschlag, D. (1999). Three metal ions at the active site of the *Tetrahymena* group I ribozyme. *Proc. Natl Acad. Sci. USA*, **96**, 12299–12304.
57. Peracchi, A., Beigelman, L., Scott, E. C., Uhlenbeck, O. C. & Herschlag, D. (1997). Involvement of a specific metal ion in the transition of the hammerhead ribozyme to its catalytic conformation. *J. Biol. Chem.* **272**, 26822–26826.
58. Moore, M. J. & Sharp, P. A. (1992). Site-specific modification of pre-mRNA: the 2′-hydroxyl groups at the splice sites. *Science*, **256**, 992–997.
59. Loria, A. & Pan, T. (1997). Recognition of the T stem-loop of a pre-tRNA substrate by the ribozyme from *Bacillus subtilis* ribonuclease P. *Biochemistry*, **36**, 6317–6325.
60. Christian, E. L., Kaye, N. M. & Harris, M. E. (2000). Helix P4 is a divalent metal ion binding site in the conserved core of the ribonuclease P ribozyme. *RNA*, **6**, 511–519.
61. Hansen, A., Pfeiffer, T., Zuleeg, T., Limmer, S., Ciesiolka, J., Feltens, R. & Hartmann, R. K. (2001). Exploring the minimal substrate requirements for trans-cleavage by RNase P holoenzymes from *Escherichia coli* and *Bacillus subtilis*. *Mol. Microbiol.* **41**, 131–143.
62. Kaye, N. M., Christian, E. L. & Harris, M. E. (2002). NAIM and site-specific functional group modification analysis of RNase P RNA: magnesium dependent structure within the conserved P1–P4 multihelix junction contributes to catalysis. *Biochemistry*, **41**, 4533–4545.
63. Busch, S., Kirsebom, L. A., Notbohm, H. & Hartmann, R. K. (2000). Differential role of the intermolecular base-pairs G292-C(75) and G293- C(74) in the reaction catalyzed by *Escherichia coli* RNase P RNA. *J. Mol. Biol.* **299**, 941–951.
64. Narlikar, G. J. & Herschlag, D. (1997). Mechanistic aspects of enzymatic catalysis: lessons from comparison of RNA and protein enzymes. *Annu. Rev. Biochem.* **66**, 19–59.
65. Pyle, A. M., Moran, S., Strobel, S. A., Chapman, T., Turner, D. H. & Cech, T. R. (1994). Replacement of the conserved G.U with a G-C pair at the cleavage site of the *Tetrahymena* ribozyme decreases binding, reactivity, and fidelity. *Biochemistry*, **33**(46), 13856–13863.
66. Herschlag, D. (1992). Evidence for processivity and two-step binding of the RNA substrate from studies of J1/2 mutations of the *Tetrahymena* ribozyme. *Biochemistry*, **31**, 1386–1399.
67. Bevilacqua, P. C., Kierzek, R., Johnson, K. A. & Turner, D. H. (1992). Dynamics of ribozyme binding of substrate revealed by fluorescence-detected stopped-flow methods. *Science*, **258**(5086), 1355–1358.

Edited by J. Doudna

(Received 23 August 2004; received in revised form 20 October 2004; accepted 27 October 2004)